



# Selective methoxylation of $\alpha$ -pinene to $\alpha$ -terpinyl methyl ether over $Al^{3+}$ ion-exchanged clays



C. Catrinescu<sup>a,b,\*</sup>, C. Fernandes<sup>a,c</sup>, P. Castilho<sup>a</sup>, C. Breen<sup>d</sup>

<sup>a</sup> Centro de Química da Madeira (CQM), Centro de Ciências Exactas e da Engenharia da Universidade da Madeira, Campus Universitário da Penteada, 9000-390 Funchal, Portugal

<sup>b</sup> “Gheorghe Asachi” Technical University of Iasi, Faculty of Chemical Engineering and Environmental Protection, Department of Environmental Engineering and Management, 73 D. Mangeron Blvd, 700050 Iasi, Romania

<sup>c</sup> Laboratório Regional de Engenharia Civil, Rua Agostinho Pereira de Oliveira, 9000-264 Funchal, Portugal

<sup>d</sup> Materials and Engineering Research Institute, Sheffield Hallam University, Howard Street, Sheffield S1 1WB, UK

## ARTICLE INFO

### Article history:

Received 22 July 2014

Received in revised form 10 October 2014

Accepted 17 October 2014

Available online 26 October 2014

### Keywords:

Ion-exchanged clays

Clay acidity

Catalysis

Pinene

Methoxylation

Terpinyl methyl ether

## ABSTRACT

In this study, we report the use of clay-based catalysts in the methoxylation of  $\alpha$ -pinene, for the selective synthesis of  $\alpha$ -terpinyl methyl ether, TME. The main reaction products and intermediates were identified by GC–MS. The reaction conditions (stirring rate and catalyst load) that afford a kinetic regime were established. SAZ-1 (Cheto, Arizona, USA) source clay and a montmorillonite (SD) from Porto Santo, Madeira Archipelago, Portugal, were modified by ion-exchange with  $Al^{3+}$  to produce catalysts with markedly different acidities and textural properties. The catalysts based on the high layer-charge SAZ-1 montmorillonite proved to be the most active. Ion-exchange with  $Al^{3+}$ , followed by thermal activation at 150 °C, afforded the highest number of Brønsted acid sites – a significant proportion of which were located in the clay gallery – and this coincided with the maximum catalytic activity. The influence of various reaction conditions, to maximize  $\alpha$ -pinene conversion and selectivity, was studied over AlSAZ-1. When the reaction was performed for 1 h at 60 °C, the conversion reached 65% with 65% selectivity towards the mono-ether, TME. Similar conversions and selectivities required up to 50 h over zeolites and other solid acid catalysts. The kinetic dependencies of this reaction on temperature and reagent concentration, over the selected clays were also investigated. It was established that, in the temperature and reagent concentration regime studied, the reaction was first order with respect to  $\alpha$ -pinene. The apparent activation energies over the two catalysts, calculated from Arrhenius plots, were almost identical at 72 kJ mol<sup>-1</sup>.

© 2014 Elsevier B.V. All rights reserved.

## 1. Introduction

The use of renewable feedstocks, such as monoterpenoids, to produce fine chemicals via heterogeneous catalytic processes is considered a sustainable approach which conforms with the principles of green chemistry [1]. Terpenes, such as limonene and pinene, are an abundant renewable feedstock, used as starting materials for the synthesis of fine chemicals, in food, cosmetic and pharmaceutical industries. Terpenes are found not only in several essential oils but also as the major constituents of pine resins and of some byproducts of the pulp, paper and food (citrus) industries [2,3]. Pinene is a natural bicyclic monoterpene that can be separated,

by steam distillation, from gum and sulphate turpentine which presents two structural isomers ( $\alpha$ - and  $\beta$ -).  $\alpha$ -Pinene is the most widely encountered terpenoid in nature [2] and finds numerous uses in the food, fragrance and pharmaceutical sectors as well as in the synthesis of chemical intermediates. Thus,  $\alpha$ -pinene is considered a versatile building block for the synthesis of high-value added chemicals, mainly through catalytic processes, such as isomerization, epoxidation and pinene oxide isomerization, hydration and dehydroisomerization, esterification, etherification [2–4] and also in a four-step synthesis of linalool from  $\alpha$ -pinene [6,10]. The alkoxylation of pinene is a less explored route to produce 1-methyl-4-( $\alpha$ -alkoxyisopropyl)-1-cyclohexenes. These compounds are used as flavours and fragrances for perfume and cosmetic products, as additives for pharmaceuticals and agricultural chemicals, and also in the food industry. Among these functionalized monoterpenes, the  $\alpha$ -terpinyl methyl ether is of commercial interest due to its pleasant grapefruit-like aroma. This compound is conventionally produced via the alkoxylation of pinene or limonene using mineral acids. The use of strong homogeneous liquid acids

\* Corresponding author at: “Gheorghe Asachi” Technical University of Iasi, Faculty of Chemical Engineering and Environmental Protection, Department of Environmental Engineering and Management, 73 D. Mangeron Blvd, 700050 Iasi, Romania. Tel.: +40 232 237594; fax: +40 232 237594.

E-mail addresses: [ccatrine@ch.tuiasi.ro](mailto:ccatrine@ch.tuiasi.ro), [ccatrine@uma.pt](mailto:ccatrine@uma.pt) (C. Catrinescu).

is not recommended for industrial applications due to the associated corrosion and environmental challenges. Previous studies on  $\alpha$ -pinene and limonene methoxylation have been principally performed using zeolites [7] although clay-based catalysts can also be used [8]. The alkoxylation of limonene over  $\beta$  zeolite and ion-exchanged clays afforded good yields (around 85%) whereas the methoxylation of pinene, over the same  $\beta$  zeolite, gave lower yields (50%) of the same product. The methoxylation of pinene has been also studied over acidic cation exchange resins [9] and sulphonic acid-modified mesoporous silica [10]. However, more recent studies over poly(vinyl alcohol) containing sulfonic acid groups [11], heteropolyacids immobilized on silica [12] and microporous and mesoporous carbons [13] reported good selectivities, of ca. 60%, at almost complete conversion.

Clay minerals, which are natural materials that cost significantly less than the catalysts listed above, are versatile and environmentally friendly catalysts that can be modified with relative ease to promote a wide variety of organic reactions [14]. Beside the type of clay, the nature, the locality and the extent of the isomorphic substitution strongly influences the layer charge of the clay and exerts a major influence on the acidity and accessibility of the active sites. These intrinsic characteristics of the clays, responsible for their catalytic activity, can be readily improved using different methods such as *ion-exchange*, *acid treatment and pillaring* [15]. Thus,  $\text{Ni}^{2+}$ - and  $\text{Al}^{3+}$ -exchanged montmorillonites, following appropriate thermal activation procedures, are considered model Lewis and Brønsted acids, respectively. The nature of the active sites has been unequivocally determined using FT-IR spectra of adsorbed pyridine [16] and verified by catalytic data.

In this work we report the synthesis of  $\alpha$ -terpinyl methyl ether via the methoxylation of  $\alpha$ -pinene over clay catalysts. Based on our recent results detailing the methoxylation of limonene [8], two starting clays, with different compositions and properties, were selected and these were activated by ion-exchange with  $\text{Al}^{3+}$  and then thermally activated at 150 °C. This approach is known to afford the maximum catalytic activity in Brønsted acid catalysed organic reactions involving polar reagents.

## 2. Experimental

### 2.1. Catalyst preparation

SAz-1 (Cheto, Arizona, USA), received from The Clay Mineral Society Source Clay repository (Purdue University), was suspended in deionized water and the  $<2\ \mu\text{m}$  size fraction was collected by centrifugation. The raw bentonite (SD) was collected from the Serra de Dentro deposit (Porto Santo - Madeira Archipelago, Portugal) and purified [17,18] to give the Na-exchanged form (NaSD). The major impurities were removed by low speed centrifugation (6 min, at 600 rpm), to obtain the  $<2\ \mu\text{m}$  size fraction, followed by the removal of inorganic carbonates by incremental addition of a 0.5 M sodium acetate buffer until the clay suspension reached pH 6.8. Then, the product was converted into the Na-exchanged form using 1 M aqueous sodium chloride solution. Excess  $\text{Cl}^-$  was removed by dialysis and the solid clay was obtained after drying the gel collected following centrifugation at 4500 rpm for 30 min. The chemical composition for SAz-1 and NaSD is reported in Table 1.

SAz-1 and NaSD were treated three times with 0.3 M  $\text{Al}(\text{NO}_3)_3$ , washed, dried and ground to give the ALSAz-1 and AISD catalysts. These samples were stored in a desiccator over saturated aqueous  $\text{Ca}(\text{NO}_3)_2$ .

### 2.2. Characterization

The XRD patterns were recorded using a Shimadzu LabX XRD-6000 diffractometer with  $\text{Cu K}\alpha$  radiation ( $\lambda = 1.54184\ \text{Å}$ ).

**Table 1**

Elemental composition for the purified host clays and for the  $\text{Al}^{3+}$  ion-exchanged forms.

Clay	Chemical composition, % oxide							
	Na	Mg	Al	Si	K	Ca	Ti	Fe
NaSD	2.6	3.4	20.5	57.4	0.9	0.5	3.3	10.3
SAz-1	0.1	6.7	20.0	59.7	0.2	3.2	0.3	1.8
AISD	0.1	2.9	22.5	54.4	0.8	0.1	5.0	12.8
ALSAz-1	0.1	6.3	23.2	68.1	0.1	0.0	0.3	1.7

The nitrogen adsorption–desorption isotherms at  $-196\ ^\circ\text{C}$  were determined on an Autosorb iQ from Quantachrome Instruments, equipped with turbomolecular pumps for high vacuum attainment, using helium (for dead space calibration) and nitrogen of 99.999% purity. Prior to the adsorption measurements, all the samples were outgassed for 5 h at 200 °C, achieved using a heating rate of  $1\ ^\circ\text{C min}^{-1}$ .

TG data were recorded on a Mettler TG50 thermobalance equipped with a TC10A processor. Samples ( $\sim 10\ \text{mg}$ ) were transferred directly out of cyclohexylamine (CHA) vapour into the thermobalance and the desorption traces were recorded at a heating rate of  $20\ ^\circ\text{C}$  under a nitrogen flow of  $25\ \text{cm}^3/\text{min}$ . Samples were conditioned for 15 min under flowing nitrogen to reduce the amount of physisorbed CHA. Variable temperature diffuse reflectance infrared Fourier transform spectra (VT-DRIFTS), were recorded at room temperature, then at  $25\ ^\circ\text{C}$  increments until 250 °C. Samples were held at a specific temperature for 15 min in a flow of dry nitrogen in a variable-temperature cell (Graseby-Specac; maximum operating temperature 500 °C). The spectrometer used was a Mattson Polaris operating at  $4\ \text{cm}^{-1}$  resolution and 256 scans.

### 2.3. Catalytic tests

$\alpha$ -Pinene and n-decane (internal standard) received from Sigma Aldrich were dried over anhydrous magnesium sulphate prior to use. Anhydrous methanol was used as received from Sigma Aldrich. The reactions were performed in a stirred 25 ml batch reactor, equipped with a reflux condenser, under drying tube ( $\text{CaCl}_2$ ) protection. Before the reaction, a known amount of catalyst was thermally activated at 150 °C, in air, for 2 h in a vial. Before being removed from the oven, the vials were stoppered and then placed in a desiccator to cool and prevent rehydration. After being cooled at room temperature (15 min) the catalyst powder was quickly transferred into the reaction vessel containing dry methanol, preheated at the reaction temperature. The injection of pinene and n-decane (internal standard) marked the start of the reaction. Samples were taken periodically and the catalyst was removed by syringe filtration. The filter had no influence on the reaction products and no further reaction took place during storage. The reaction products were identified by GC–MS (Agilent 6890N/MSD GC–MS system) and quantified by GC with FID, using a J&W Carbowax 20 M column and n-decane as an internal standard.

In a separate test the effect of the larger amounts of water available in non-thermally activated clays was evaluated. These high water content samples were stored in a desiccator over saturated aqueous  $\text{Ca}(\text{NO}_3)_2$  prior to their use as a catalyst.

Initial reaction rates were calculated utilizing the concentration versus time data collected during the first few minutes of the reaction. During this initial time period, the concentration of the reactants decreased almost linearly with time, and hence the reaction rate i.e., the differential of the reactant concentration with respect to time, was calculated from the slope of a linear fit to these initial data.

**Table 2**The main characteristics of the Al<sup>3+</sup>-exchanged clays.

Clay	$d_{001}$ , Å	$A_{SBET}$ , m <sup>2</sup> g <sup>-1</sup>	Acidity, mmol H <sup>+</sup> g <sup>-1</sup> clay	CEC, meq 100 g <sup>-1</sup>
Al-SD	14.8	140	1.2	81
Al-SAZ-1	14.8	96	1.64	120

### 3. Results and discussion

#### 3.1. Characterization

The chemical analysis of the original and ion-exchanged clays (Table 1) confirmed that SAz-1 contained a large amount of structural magnesium – located in the octahedral sheet – and, in comparison to SD, exhibited a higher cation exchange capacity (CEC) which reflected a higher layer charge. The purified SD sample is an iron-rich clay that displayed a markedly higher specific surface area than SAz-1. The most important results of the physical-chemical characterization are summarized in Table 2.

The XRD trace of the unpurified SD confirmed that the major components were montmorillonite and magnesian calcite (C). Smaller amounts of anorthite (A), feldspar (F) and quartz (Q) were present as impurities (Fig. 1). However, most of the impurities were removed during the purification step, as shown in the trace obtained from NaSD. The powder XRD patterns of the Al<sup>3+</sup>-exchanged clays revealed peaks corresponding to montmorillonites, with well defined  $d_{001}$  reflections ( $5.96^\circ$   $2\theta$ , 14.8 Å), suggesting a well-ordered arrangement of the clay platelets, with two layers of hydration water in the interlayer prior to activation at 150 °C.

The textural properties of Al<sup>3+</sup>-exchanged clays were investigated using nitrogen adsorption at –196 °C. The values of the specific surface areas, obtained by applying the B.E.T. method [23] to the corresponding isotherms, are presented in Table 2. These represent the accessible surface in the unswollen state of the clay and is determined by the microporosity resulting from the quasi-crystalline overlap region and from the accessible areas of the interlayer [8]. The total specific surface area might also be affected,

to a smaller extent, by the arrangement of the particles with respect to each other (microstructure). Previous work revealed that the isotherms for Al-SD and Al-SAZ-1 approached type IIb [8] and displayed hysteresis loops associated with slit shaped pores between plate-shaped particles. The high surface areas were attributed to the presence of narrow micropores [8].

The nature of the acid sites generated on the Al<sup>3+</sup>-exchanged clays were explored by comparing the variable temperature diffuse reflectance infrared Fourier transform spectra (VT-DRIFTS) of pyridine-treated samples and the number of sites were estimated using thermal desorption (TG) of cyclohexylamine (CHA). In accordance with our previous studies [8,16,20], Al<sup>3+</sup>-exchanged clays exhibited bands at 1635 and 1540 cm<sup>-1</sup> attributed to pyridinium ion, formed on Brønsted acid sites (BPYR), and some minor bands at 1613 and 1450 cm<sup>-1</sup> that are diagnostic for pyridine co-ordinately bound to Lewis acid sites (LPYR). The peaks at 1596 and 1440 cm<sup>-1</sup>, in the spectra recorded at lower temperatures, report the presence of H-bonded pyridine (HPYR). All these species contribute to the intensity of the 1490 cm<sup>-1</sup> band although the largest contribution at higher temperatures (>120 °C) is from BPYR.

The evolution of these diagnostic bands with temperature is presented in Fig. 2. The spectrum recorded at 50 °C for pyridine-treated Al<sup>3+</sup>-exchanged samples revealed an already well-defined BPYR peak at 1539 cm<sup>-1</sup>. This peak increased in intensity and reached a maximum at 150 °C, then diminished progressively for activation at higher temperatures. The continued presence of this band at 250 °C highlighted the strength of the Brønsted acid sites on Al<sup>3+</sup>-exchanged clays. The spectrum of pyridine-treated Al-SD at 150 °C exhibited strong bands, diagnostic of pyridine bound to Brønsted acid sites, at 1490, 1540 and 1653 cm<sup>-1</sup> [8,16].

Thermal desorption of cyclohexylamine was used to quantify the number of the acid sites on clay catalysts [16]. The technique determines the weight loss between 280 and 440 °C and converts it to the number of mmol of CHA desorbed. The relative ease of obtaining this quantity has popularized its use, even though the value obtained does not readily distinguish between cyclohexylamine bound to Brønsted or Lewis acid sites [20]. The quantity of CHA desorbed from Al-SD, in the appropriate temperature interval

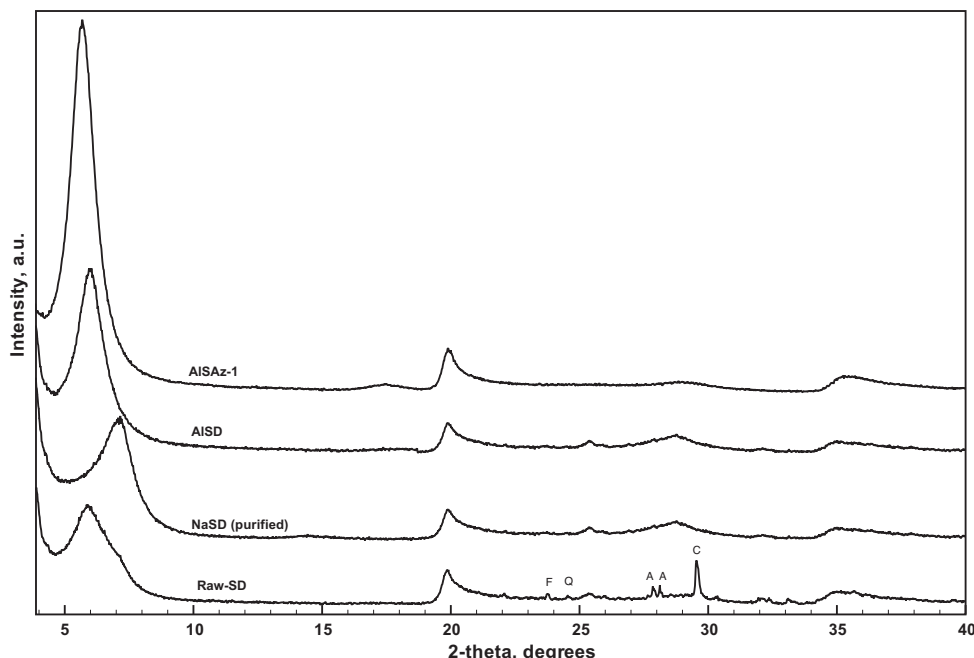


**Fig. 1.** The powder XRD patterns for raw, purified and Al<sup>3+</sup>-exchanged clays. Impurities: magnesian calcite (C), anorthite (A), feldspar (F) and quartz (Q).

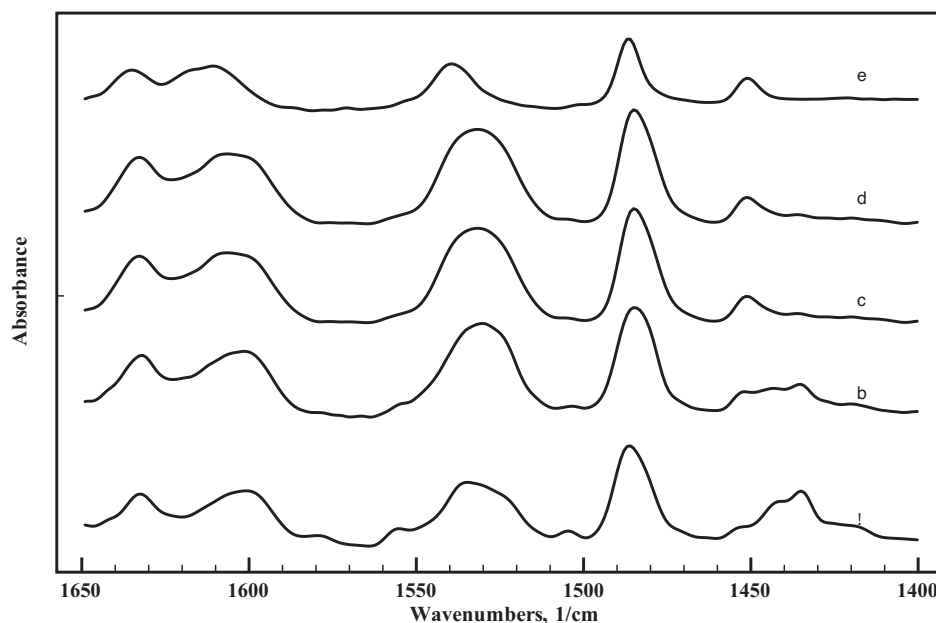


Fig. 2. VT-DRIFTS spectra of Al-SAZ-1 following exposure to pyridine vapour and evacuation at (a) 50 °C, (b) 100 °C, (c) 150 °C, (d) 200 °C and (e) 250 °C.

(Table 2) was lower than that desorbed from Al-SAZ-1, which correlated well with the difference in CEC between SAZ-1 (120 meq 100 g<sup>-1</sup>) and SD (81 meq 100 g<sup>-1</sup>).

A significant difference between SAZ-1 and SD is the extent of replacement of aluminium by magnesium in the octahedral layer, resulting in different layer charges which are identified by the different cation exchange capacities (CEC) and acidities, as shown in the last two columns in Table 2. The location and the density of the layer charge are the main characteristics that are expected to influence the catalytic activity, provided that the interlayer space is accessible to the reagents.

## 3.2. Catalytic tests

### 3.2.1. Potential mass transfer limitations

A preliminary investigation was conducted to identify the experimental conditions that ensure a true kinetic regime for the tests, i.e. the absence of external mass transfer limitations. Initial rate measurements were carried out at different stirring rates, catalyst loadings and temperatures. The extent of the external diffusion has been verified by performing experiments at increasing stirring rates (100, 250, 500 and 750 and 1000 rpm at 60 °C). The reaction rate increased up to 500 rpm then approached an asymptotic value beyond which the external mass transfer effects were negligible.

Having adopted a reaction temperature of 60 °C and a stirring rate of 750 rpm, the kinetic regime was confirmed by performing experiments at increasing catalysts loads. The absence of mass transfer limitations at this temperature also guaranteed their absence at lower temperatures, where the reaction was slower. The experimental results were plotted using  $1/r = f(1/m)$  charts (Fig. 3), where  $r$  is the reaction rate and  $m$  is the mass of catalyst used [21,22]. The plots were linear, for 0.50–4.0% (w/v) range, and passed through the origin, confirming that the mass transfer resistance was negligible in this range. The value of the reaction rate per unit catalyst mass ( $3 \times 10^{-6} \text{ mol s}^{-1} \text{ g}^{-1}$ ) was constant over this interval and decreased to values below  $2 \times 10^{-6} \text{ mol s}^{-1}$  at catalyst loadings in excess of 10% w/v. Significantly lower reaction rates ( $<10^{-7} \text{ mol s}^{-1} \text{ g}^{-1}$ ) were reported by Pito et al. [11,12] and Matos [13] in catalytic tests performed over extended reaction time, of 30–60 h.

### 3.2.2. Reaction products and intermediates

Scheme 1 illustrates the main reaction products and intermediates identified using GC–MS (Supporting information). Pinene (1) reacted with methanol over the acid sites available on the clay surface to form terpinyl methylether, TME, (8) as the main reaction product. Other compounds were also identified in the complex reaction mixture and the most important intermediates were identified as: (i) bi-cyclic terpenes: camphene (9) and unreacted pinene (1); (ii) monocyclic terpenes: limonene (5), terpinolene (6) and terpinene (7), and (iii) bicyclic ethers ( $\alpha$ -fenchyl methyl ether, and bornyl methylethers).

In order to explain the formation of these intermediates, it is reasonable to assume that protons generated by the polarization of water [5,19,20], or methanol [8], by the small, highly-charged Al<sup>3+</sup>-cations will protonate pinene (1), leading to the pinyli ion (2). Another possibility is the generation of methoxonium ions from methanol, which will act as the protonating agent of pinene, leading to the same pinyli ion (2). Then, the acid-catalysed process proceeds via two parallel pathways: (i) ring expansion, via the bornyl ion (4), giving rise to bi- and tricyclic isomerization products (camphene, 9) and, after the addition of methanol, to bicyclic ethers (methyl fenchyl ether, 10, methyl bornyl ether, 11), and (ii) via the terpinyl ion (3), yielding monocyclic terpenes as isomerization products (limonene, 5, terpinolene, 6, terpinene, 7) and terpinyl methylethers as methoxylation products (terpinyl methylether, 8). This range of intermediates and products conforms with the reaction scheme proposed by Pito et al. [11,12].

A typical set of concentration versus time data, obtained for the alkoxylation of  $\alpha$ -pinene over Al-SAZ-1 and Al-SD catalysts, is presented in Fig. 4. This figure also presents the yield of pinene and terpinyl methylether, as a function of time elapsed, along with the content of the other products identified above. The solid lines linking the decrease in  $\alpha$ -pinene concentration at early times identify the ranges used for the calculation of the initial reaction rates, estimated as described in the experimental section.

The most important feature of this catalytic system was the high selectivity towards the main product,  $\alpha$ -terpinyl methyl ether, especially at high pinene conversions. This behaviour contrasts with that of limonene alkoxylation, when high selectivity was observed during the early stages of reaction and decreased at high

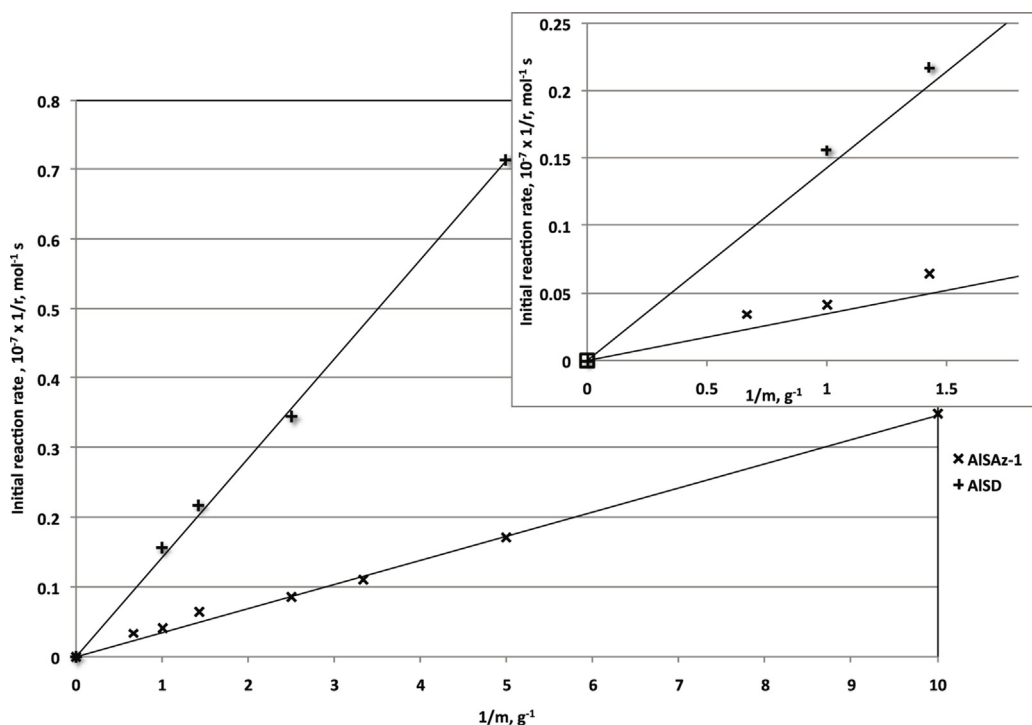


**Fig. 3.** The influence of the catalyst load on the initial reaction rate over AISAz-1 and AISD. Inset: Early time behaviour. Reaction conditions: 10 ml methanol, 0.5 ml pinene, 60 °C, 750 rpm.

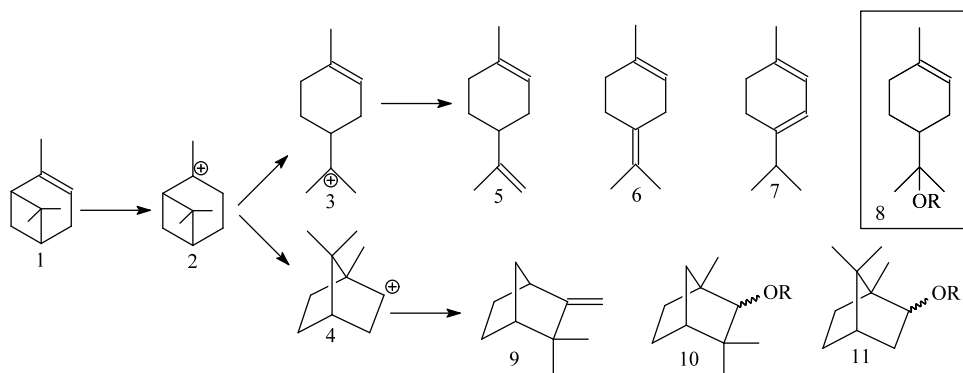
limonene conversions. The system studied here is of considerable practical importance because it offers good selectivities towards the mono-ether (65%), even at high pinene conversion (higher than 60%). Moreover, the  $\text{Al}^{3+}$ -clay catalysts were able to produce these high yields in only 1 h whereas other solid acids [11–13] required up to 50 h to produce similar results.

The data in Fig. 4 clearly demonstrate that the catalytic activity was profoundly influenced by the nature of the starting clay (SAz-1 or SD). Catalytic activities over clays, whether they arise from Brønsted or Lewis acidity, generally correlate with the cation-exchange capacity (CEC) of the base clay, provided the reactant can enter the gallery. Thus, SAz-1, a well-known montmorillonite of relatively high CEC (120 meq (100 g clay)<sup>-1</sup>), would provide more acid sites than a similarly exchanged SD sample (CEC 81 meq (100 g clay)<sup>-1</sup>). The catalytic activities recorded in this reaction clearly reflected the relative abundance of acid sites on the catalyst surface. Thus, for these  $\text{Al}^{3+}$ -exchanged clays the order of activities was the same as the order of acid site concentrations, as determined by CHA desorption experiments (Table 2), which were also related to the CEC of the selected clay.

The selectivity towards  $\alpha$ -terpinyl methyl ether (Fig. 4) was similar, irrespective of the nature of the host clay, suggesting that the same mechanism was operating in both cases. This is consistent with the proposed model, with protons being produced from water molecules that have been strongly polarized by the exchangeable  $\text{Al}^{3+}$ -cations present in the interlayer space of the clay [8,16,19,20].

### 3.2.3. Influence of the thermal activation temperature

Fig. 5, which presents the pinene conversion over AISAz-1 catalyst pretreated at different temperatures, supported the generally accepted model that the acid character of an  $\text{Al}^{3+}$ -exchanged montmorillonite is strongly dependent on the thermal activation procedure. The deliberately hydrated samples, displayed a very low catalytic activity, suggesting that the acid sites were blocked by water making them inactive towards the reactants. Increasing the pretreatment temperature to 80 and 100 °C caused a marked increase in activity. The maximum Brønsted acidity was generated upon thermal activation at 150 °C, as shown in the VT-DRIFTS spectra of the pyridine treated  $\text{Al}^{3+}$ -clays, but only a slight increase in activity was observed at this temperature. Increasing the thermal



**Scheme 1.** The main reaction products and intermediates identified by GC-MS in the reaction mixture.

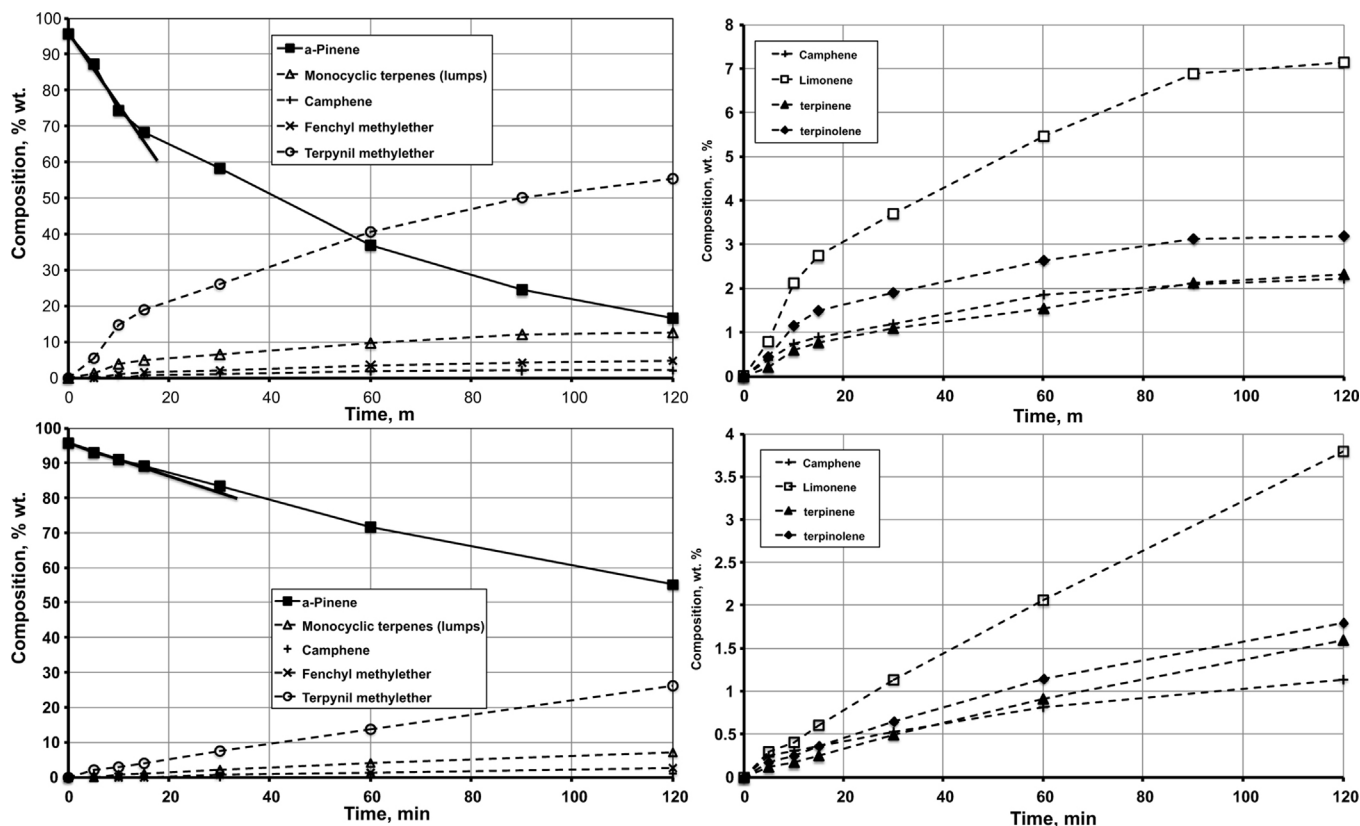


**Fig. 4.** The change in composition of the reaction mixture during pinene methoxylation over (a and b) ALSAz-1 and (c and d) ALSD. Reaction conditions: 200 mg catalyst, 10 ml methanol, 0.5 ml pinene, 60 °C.

activation temperature above 150 °C, is known to cause a reduction in the Brønsted acidity and an increase in the Lewis acidity in accordance with the model in which the exchange ions become electron pair accepting, or Lewis acid, sites as the directly coordinated water is driven off [16]. Therefore, a pretreatment temperature of 150 °C was selected for further studies, in order to avoid the uncertainty regarding the Brønsted/Lewis acid balance and to take advantage of the maximum number of the Brønsted acid sites.

The variation of selectivity towards terpinyl methylether, TME, with the extent of pinene conversion was also scrutinized. The data in Fig. 5B clearly illustrate that the activation temperature exerted little influence on selectivity, especially at low pinene conversion. Therefore, while the activation temperature exerted a considerable effect on the reaction rate, the selectivity toward TME was not influenced in any significant way.

### 3.2.4. Influence of the reaction temperature

The influence of the reaction temperature on pinene conversion and selectivity towards the mono-ether is presented in Fig. 6A and B. The catalysed reactions were carried out at different temperatures (35, 45, 55 and 65 °C) over 100 mg of Al-SAZ-1 catalyst while the pinene: methanol molar ratio and the catalyst loading were kept constant. As anticipated, pinene conversion increased with the temperature, under otherwise identical conditions. The same trend was observed for limonene conversion in a related system [8]. Increasing the temperature up to 65 °C, did not lead to a decrease in selectivity, as observed in the previous study on limonene methoxylation [8]. The selectivity to the mono-ether (Fig. 6), at constant conversion, seems to be largely unaffected by raising the reaction temperature.

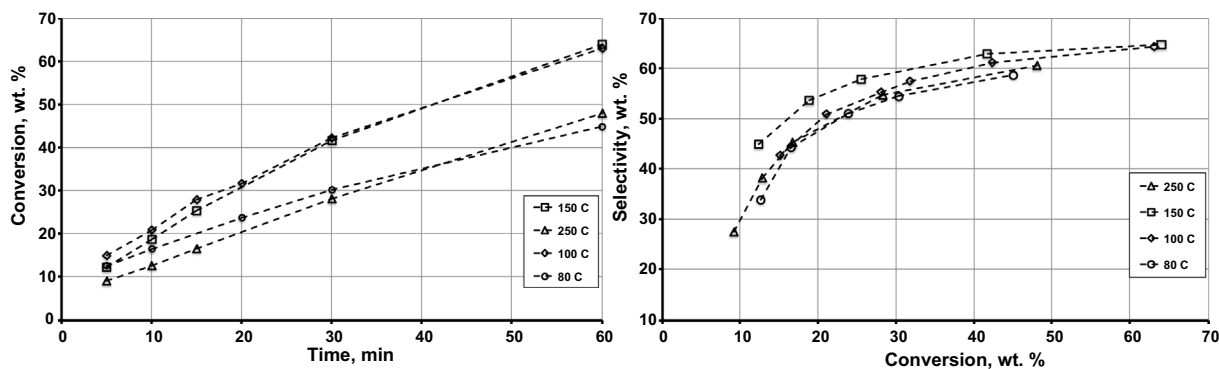


**Fig. 5.** The effect of the Al-clay activation temperature on the methoxylation of  $\alpha$ -pinene: (A)  $\alpha$ -pinene conversion vs. time and (B) the correlation selectivity vs. conversion. Reaction conditions: 200 mg cat, 10 ml methanol, 0.5 ml pinene, 60 °C.

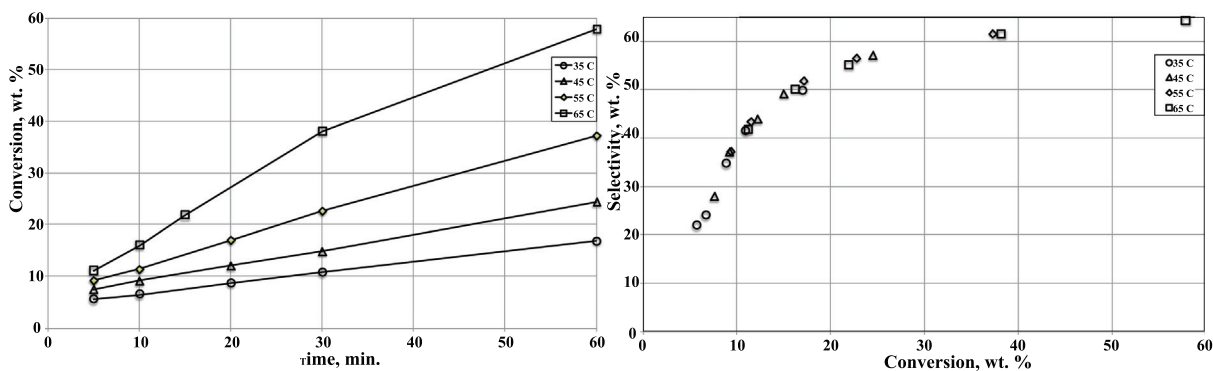


Fig. 6. The effect of the reaction temperature on the methoxylation of  $\alpha$ -pinene: (A)  $\alpha$ -pinene conversion vs. time and (B) the correlation selectivity vs. conversion. Reaction conditions: 100 mg Al-SAZ-1, 0.5 ml Pinene, 10 ml MeOH.

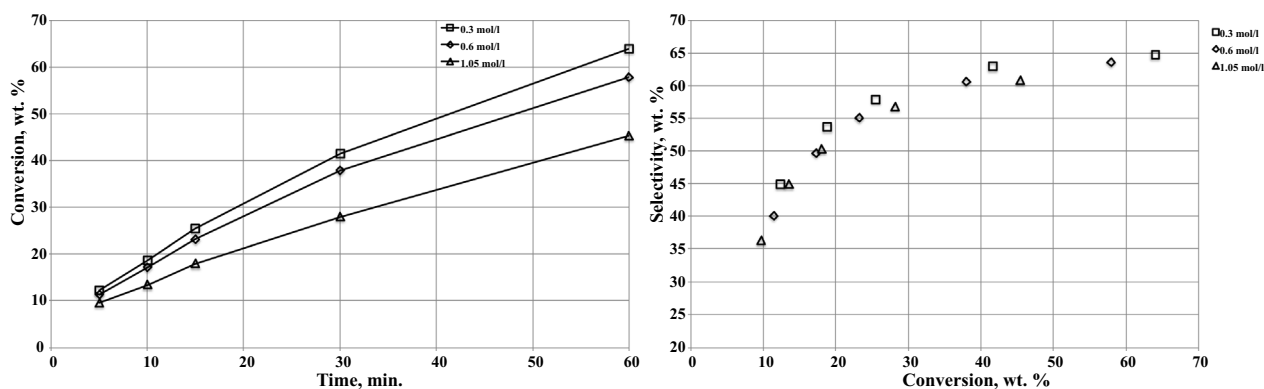


Fig. 7. The effect of the initial pinene concentration on the methoxylation of  $\alpha$ -pinene: (A)  $\alpha$ -pinene conversion vs. time and (B) the correlation selectivity vs. conversion. Reaction conditions: 200 mg catalyst, 10 ml methanol, 60 °C.

3.2.5. Influence of initial  $\alpha$ -pinene concentration

The effect of the initial  $\alpha$ -pinene concentration on the conversion and on the selectivity towards the mono-ether is presented in Fig. 7. Doubling the initial pinene concentration, from 0.3

0.6 mol/L, only caused a slight decrease in pinene conversion at a fixed reaction time; this trend was further accentuated at a higher initial concentration (1.05 mol/L). Note that the initial reaction rate was higher when the initial concentration of pinene was higher,

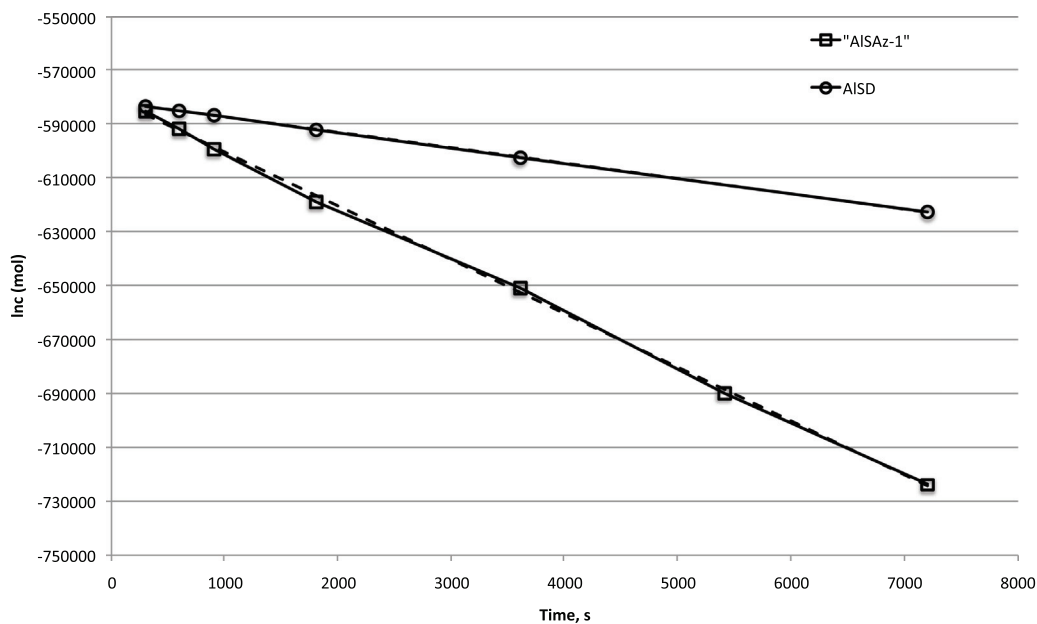


Fig. 8.  $\alpha$ -Pinene concentration versus time during the methoxylation of  $\alpha$ -pinene over AlSAz-1 and AISD. Reaction conditions: 200 mg catalyst, 10 ml methanol, 0.5 ml pinene, 60 °C.

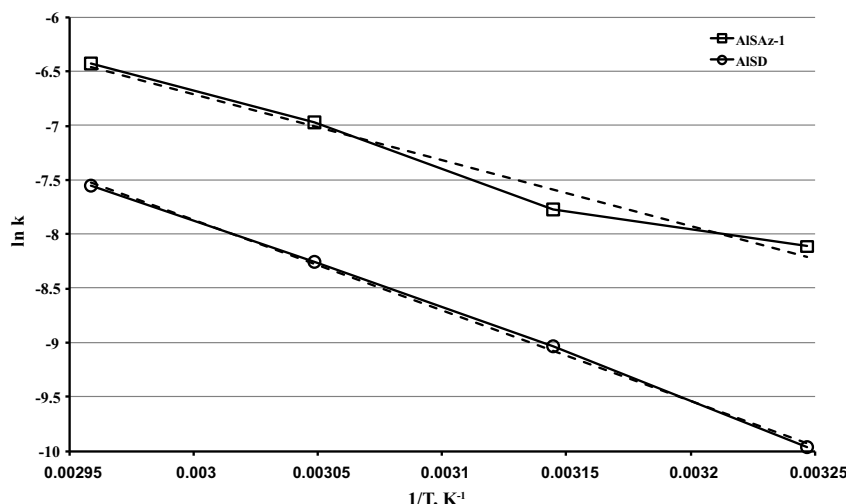


Fig. 9. Arrhenius plot for methoxylation of  $\alpha$ -pinene over AISAz-1 and AISD. Reaction conditions: 100 mg catalyst, 10 ml methanol, 0.5 ml pinene.

under otherwise identical conditions. Again, the selectivity to the mono-ether, at similar conversion, was not affected by the initial pinene concentration.

### 3.3. Kinetic study

The linear form of the logarithmic plot of  $\alpha$ -pinene concentration versus time, demonstrated that the reaction over the clay catalysts followed pseudo first-order kinetics; i.e. first order with respect to  $\alpha$ -pinene and zero-order with respect to methanol, because the latter was present in large excess. The values of the reaction rate constants, determined from the slopes of the two lines of negative slope in Fig. 8, confirmed that the rate of reaction at 60 °C was faster over AI-SD than AI-SAz.

An Arrhenius plot of these reaction rate constants is shown in Fig. 9. The slopes of the  $\ln r$  versus  $1/T$  lines were similar for both AI-exchanged clays, and an activation energy of 71.7 kJ/mol was obtained for the alkoxylation reaction.

The similarity in activation energies suggested that the difference in rate constants must be attributed to a difference in the pre-exponential factor. An acceptable explanation for the faster rate over AISD is that the significantly higher external surface area makes it easier for the reactant and product molecules to arrive at the Brønsted acid sites in the gallery. This suggests that the rate determining step involves transport from the liquid phase to the interlayer space perhaps via a 'stagnant' layer of reaction medium close to the clay surface. Alternatively, the larger distance between exchange sites in AISD, which has a lower density of exchange sites per unit surface, may control or contribute to easier access to the reaction sites in the clay interlayer. The high charge density of the AISAz sample may result in interlayer congestion which results in a slower rate of turnover at the acid sites.

## 4. Conclusion

Modified clays have been proposed as active and selective catalysts for the synthesis of  $\alpha$ -terpinyl methyl ether by alkoxylation of  $\alpha$ -pinene with methanol. The GC-MS analysis of the reaction mixtures showed that  $\alpha$ -terpinyl methyl ether was obtained with good selectivity over the Al<sup>3+</sup>-exchanged clay catalysts. AISAz-1 was significantly more active than the similarly exchanged SD, and this behaviour was rationalized taking into account the higher number of Brønsted acid sites present in this high charge clay, as shown by the acidity measurements (VT-DRIFTS and TG of CHA). The

activation temperature had a strong influence on the acidity of the clay surface and was, consequently, a significant factor in the control of the reaction rate. In addition, other reaction parameters, such as the reaction temperature and the initial concentration of  $\alpha$ -pinene could be used to optimize the catalytic activity. The selectivity towards the mono-ether at constant conversion was much less dependent on these parameters.

The most important feature of this catalytic system was the high selectivity towards the main product,  $\alpha$ -terpinyl methyl ether, especially at high pinene conversions. In this sense, the selectivity towards TME (65%), obtained over Al<sup>3+</sup>-exchanged clays, is similar to that obtained by Pito et al. [11,12] and Mato et al. [13] (60%) but at a much higher reaction rate. On the other hand, Hoelderich [7] suggested that zeolite  $\beta$  is more active than the clay-based catalysts, at the expense of the selectivity, which is significantly poorer (54%), especially at high conversions. A different trend was observed in the related alkoxylation of limonene, over the same catalysts, where the selectivity decreased as the limonene conversion progressed. The reaction followed pseudo first-order kinetics, with similar activation energies for both catalysts.

## Acknowledgements

This work was supported by Portuguese funds (FCT – Fundação para a Ciência e a Tecnologia, projects PTDC/CTM-CER/121295/2010 and PEst OE/QUI/UI0619/2011).

## Appendix A. Supplementary data

Supplementary data associated with this article can be found, in the online version, at <http://dx.doi.org/10.1016/j.apcata.2014.10.028>.

## References

- [1] P.T. Anastas, L.B. Bartlett, M.M. Kirchoff, T.C. Williamson, *Catal. Today* 55 (2000) 11–22.
- [2] Y. Noma, Y. Asakawa, in: K.H.C. Baser, G. Buchbauer (Eds.), *Handbook of Essential Oils: Science, Technology, and Applications*, CRC Press, Boca Raton, 2010, pp. 585–736.
- [3] E.V. Gusevskaya, *ChemCatChem* 6 (2014) 1506–1515.
- [4] M. Besson, P. Gallezot, C. Pinel, *Chem. Rev.* 114 (2014) 1827–1870.
- [5] A. Corma, S. Iborra, A. Velty, *Chem. Rev.* 107 (2007) 2411–2502.
- [6] P. Mäki-Arvela, B. Holmbom, T. Salmi, D.Y. Murzin, *Cat. Rev.* 49 (2007) 197–340.
- [7] K. Hensen, C. Mahaim, W.F. Hölderich, *Appl. Catal. A: Gen.* 149 (1997) 311–329.
- [8] C. Catrinescu, C. Fernandes, P. Castilho, C. Breen, M.M.L. Carrott, I.P.P. Cansado, *Appl. Catal. A: Gen.* 467 (2013) 38–46.

- [9] M. Yoshiharu, M. Masahiro, *Jpn. Kokai* 75 (1976) 948.
- [10] J.E. Castanheiro, L. Guerreiro, I.M. Fonseca, A.M. Ramos, J. Vital, *Stud. Surf. Sci. Catal.* 174 (2008) 1319–1322.
- [11] D.S. Pito, I.M. Fonseca, A.M. Ramos, J. Vital, J.E. Castanheiro, *Chem. Eng. J.* 147 (2009) 302–306.
- [12] D.S. Pito, I. Matos, I.M. Fonseca, A.M. Ramos, J. Vital, J.E. Castanheiro, *Appl. Catal. A: Gen.* 373 (2010) 140–146.
- [13] I. Matos, M.F. Silva, R. Ruiz-Rosas, J. Vital, J. Rodríguez-Mirasol, T. Cordero, J.E. Castanheiro, I.M. Fonseca, *Micropor. Mesopor. Mater.* 199 (2014) 66–73.
- [14] J.M. Adams, R.W. McCabe, *Handbook of Clay Science*, vol. 1, Elsevier, 2006, pp. 541–581 (Chapter 10.2).
- [15] F. Bergaya, B.K.G. Theng, G. Lagaly, *Handbook of Clay Science*, vol. 1, Elsevier, 2006, pp. 261 (Chapter 7).
- [16] C. Breen, *Clay Miner.* 26 (1991) 473–486.
- [17] L.J. Arroyo, H. Li, B.J. Teppen, S.A. Boyd, *Clays Clay Miner.* 53 (2005) 512–520.
- [18] S. Kaufhold, R. Dohrmann, M. Klinkenberg, S. Siegesmund, K. Ufer, *J. Colloid Interface Sci.* 349 (2010) 275–282.
- [19] C. Breen, *Clay Miner.* 26 (1991) 487–496.
- [20] P. Komadel, M. Janek, J. Madejova, A. Weekes, C. Breen, *J. Chem. Soc. Faraday Trans.* 93 (1997) 4207–4210.
- [21] T.K. Sherwood, *Pure Appl. Chem.* 10 (1965) 595–610.
- [22] H. Hichri, A. Accary, J. Andrieu, *Chem. Eng. Process.* 30 (1991) 133–140.
- [23] S. Brunauer, P.H. Emmett, E. Teller, *J. Am. Chem. Soc.* 60 (1938) 309–319.